ISBN: 978-3-95450-184-7 doi:10.18429/JACoW-IPAC2018-THPMK013

A WIGGLER MAGNET DESIGN FOR THE TPS

J. C. Jan†, Y. L. Chu, F. H. Tseng and C. S. Hwang, National Synchrotron Radiation Research Center, Hsinchu, Taiwan, R.O.C

Abstract

The Taiwan Photon Source (TPS) is an advanced 3 GeV photon source facility operating at the National Synchrotron Radiation Research Center (NSRRC). Ten insertion devices (IDs) have been installed in phase-I during 2015. Recently, plans and designs for several phase-II IDs including In-vacuum Undulators (IU), Cryogenic Undulators (CU), Elliptical Polarization Undulators (EPU) and Wiggler magnets are pursued at NSRRC and are expected to be installed before 2020. In particular, a room temperature wiggler magnet with 100 mm period length (W100), will be designed and installed for microscopy experiments. The maximum field strength of the proposed W100 is 1.8 T with four main periods and is designed to generate 5-50 keV photons for the microscopy beam line. The magnetic design and photon characteristics of the W100 together with its effects on the stored beam will be discussed in this paper.

INTRODUCTION

TPS is an advanced 3 GeV light source that provides high brilliance and high energy photon beams. Presently, there exist seven beam lines served by ten IDs, listed in Table 1. There are nine beam lines served by seven IDs and two bending magnets in the phase-II proposal. One of the IDs is a high field wiggler magnet expected to provide high energy photons up to 50 keV. The TPS accelerator consists of a Double-Bend Achromat (DBA) lattice and provides an emittance of 1.6 nm·rad in normal low emittance mode of operation [1,2]. The emittance and energy spread of the TPS is expected to be increased by the proposed high field insertion device (W100) in the low emittance mode [3]. Thus, a high field wiggler magnet needs to be short to avoid excessive emittance increase and can therefore share the straight section with a SRF cavity.

The low energy ring, the Taiwan Light Source (TLS, 1.5 GeV), is still operating and fully open to user, simultaneously with TPS. The TLS provides VUV, IR, soft and hard x-rays from bending magnets, EPU, planar undulators, as well as traditional and superconducting wiggler magnets. The beam lines and end stations of the TLS are expected to be moved to the TPS, thus eliminating superconducting magnets of LHe bath type in the future. Therefore, superconducting magnets in TLS will be replaced by room temperature wiggler magnets or bending magnets in the TPS.

Table 1: IDs and Beam Lines in the TPS

	No	Photon source	Energy (keV)
Phase I (implemented in 2015)	05A	IU22-3m	5.7-20
	09A	IU22 × 2	5.6-25
	21A	IUT22-3m	7-25
	23A	IU22-3m	4-15
	25A	IU22 × 2	5.5-20
	41A	EPU48 × 2	0.4-1.2
	45A	EPU46	0.28-1.5
Phase II (in preparation)	07A	IU22-3m	5.7-20
	13A	IU24-4m	4-23
	15A	CUT	8-35
	19A	CU15-2m	10-40
	31A	W100	5-50
	24A	BM	0.2-3
	27A	EPU66	LP: 0.09-2.5 CP: 0.09-1.2
	39A	EPU168	0.02-0.3
	44A	BM	4.5-34

STRUCTURE AND PARAMETERS OF THE W100

The parameters of the W100 are listed in Table 2. The period length is 100 mm and the maximum field strength is 1.8 T in a 14 mm magnetic gap. The W100 is of the hybrid design composed of Vanadium Permendur steel (VP) poles and NdFeB permanent magnet material (PM) as shown in Fig. 1. The magnet model includes the permanent end blocks (end PM), end poles, main permanent blocks (main PM), main poles and side permanent blocks (side PM). The pole tips protrude the PM blocks by 1 mm. The side PM blocks were added to extend the good field region (GFR) of the W100. The asymmetric field distribution was generated by an even pole number design that ensures that the first field integral is zero. A pair of end poles and end PMs was designed to minimize the trajectory offset when the electron beam passes through the W100. The trajectory offset will be optimized by the thickness of the end PM and end poles.

A comparison of the photon fluxes from the W100 (TPS-W100), the TPS-bending magnet (TPS-BM) and superconducting wiggler (TLS-SW60) are shown in Fig. 2. Here, the field strength of the TLS-SW60 and TPS-BM is 3.2 T and 1.19 T, respectively. The flux of TPS-W100 is higher than TLS-SW60 and TPS-BM that especially at a high photon energy of 50 keV, higher by two orders of magnitude.

† janjc@nsrrc.org.tw

Content from this work may be used under the terms of the CC BY 3.0 licence (© 2018). Any distribution of this work must maintain attribution to the author(s), title of the work, publisher, and DOI.

ISBN: 978-3-95450-184-7 doi:10.18429/JACoW-IPAC2018-THPMK013

Content from this work may be used under the terms of the CC BY 3.0 licence (© 2018). Any distribution of this work must maintain attribution to the author(s), title of the work, publisher, and DOI.

Table 2: W100 Parameters

W100 parameters	
Peak field strength	1.8 T
Period length	100 mm
Number of main periods	4
Pole material	Vanadium Permendur steel
Main pole size	$75\times60\times15.3$ mm^3
Permanent magnet, PM	NdFeB
Main PM size	$115\times69\times34.7$ mm^3
Side PM size	$20\times60\times15.3$ mm^3
Pole gap	14 mm
Deflection parameter, k	16.91
Critical Energy	10.8 keV
Total radiation power	3.7 kW
Power density	3.11 kW/mrad^2

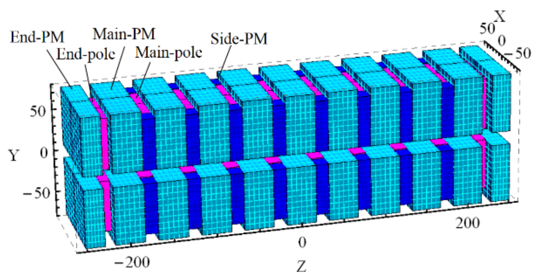

Figure 1: Structure of the W100.

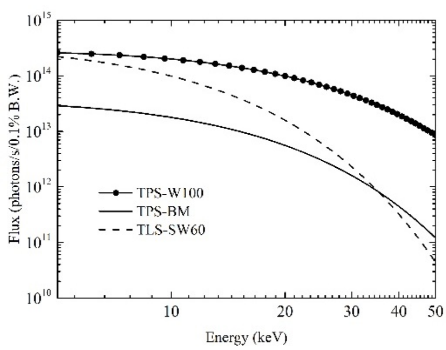

Figure 2: Spectra comparisons for the TPS-W100, TPS-BM and TLS-SW6.

MAGNETIC CIRCUIT

The magnetic circuit of the W100 was simulated by the RADIA and TOSCA program. Vanadium Permendur steel (Fe: 49 %, Co: 49 %, V: 2 %) is used for the pole material and NdFeB for the permanent magnet blocks (remanent magnetization 1.25) in the RADIA code. The field distribution (By), electron beam angle (first field integral, IBy) and trajectory (second field integral, IIBy) for the W100 are shown in Fig. 3 where the longitudinal scale is the same for model and field distribution. The peak fields, marked by a, b and c, are determined by the edge of the PM end block, the center of the end pole and the center of the first main pole, respectively. The integral IBy is always zero due to the even pole number while. IIBy can be optimized by the thickness of the end PM block and end pole because the fields of the PM end block and end pole are of opposite sign, (shown as label a and b in Fig. 3).

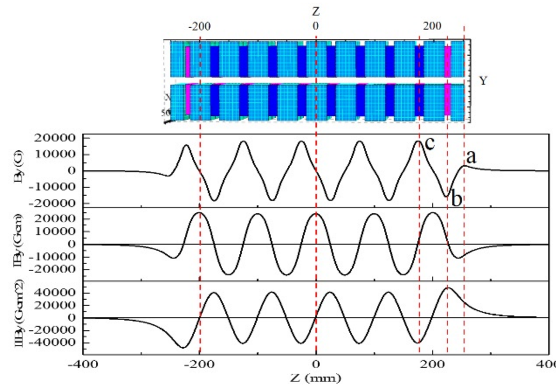

Figure 3: Field distribution for the W100.

Figure 4 (a) and (b) display the vertical field By and IIBy as obtained by the RADIA and TOSCA programs. In the TOSCA program, the coercive force (Hcb) is set to 995 (kA/m). The model definition and mesh sizes in RADIA and TOSCA are different and the peak field calculated by TOSCA is 0.5 % higher compared to that from RADIA. The difference in the integral IIBy between the RADIA and TOSCA simulation is 4717 G·cm^2. This difference in IIBy can be easily compensated by adjusting the end pole position along the y-direction. The integral IIBy increases by 8500 G·cm^2 while moving the end pole by only 0.2 mm. Thus, the integral IIBy will be corrected by adjusting of the end pole as determined by field measurements. These results demonstrate that the model definition and parameter setting are correct in both program.

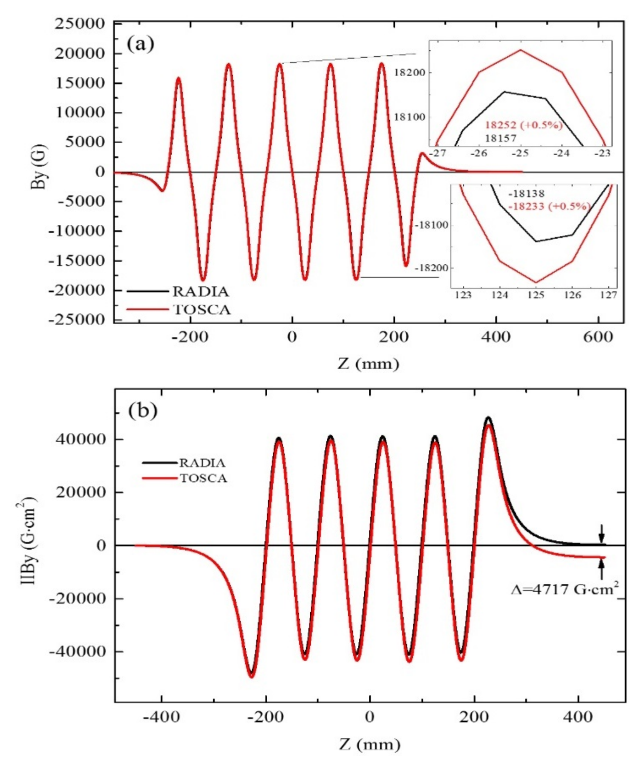

Figure 4: Comparison of the field distribution (a) and electron beam trajectory (b) as calculated by RADIA and TOSCA.

ISBN: 978-3-95450-184-7 doi:10.18429/JACoW-IPAC2018-THPMK013

Figure 5 (a) and (b) show the field distribution and field homogeneity (ΔBy/By) along transverse direction at the central pole. The ΔBy/By is less than 1.5 % and 0.1 % in a transverse good field region (GFR) of ±25 mm and ±9.5 mm, respectively. A 2 mm deep and 45° chamfer cut are required to secure the PM block during the assembly. A comparison between a 2 mm (5 mm) chamfer and no chamfer shows that the field strength is reduced by 0.04 % (0.1 %) while effects on the GFR are negligible.

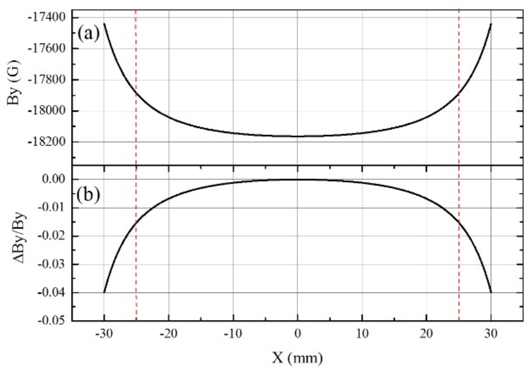

Figure 5: Field distribution (a) and field homogeneity (b) in the transverse direction at the central pole of the W100.

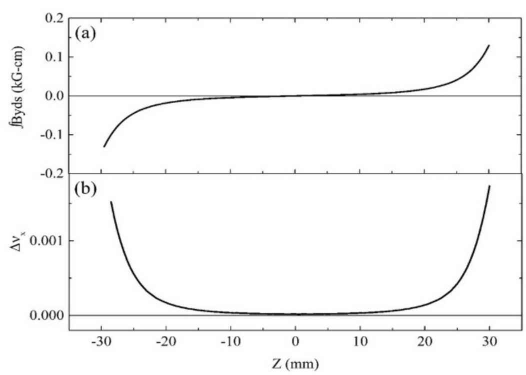

Figure 6: Dynamic field integral (a) and tune shift (b) as a function of the electron beam offset in the W100.

A refined analysis was done to show the field integral along the actual (swing) trajectory of of electron beam [4]. Figures 6 (a) and (b) display the field integrals along the dynamic trajectory and the electron beam tune shift due to the W100 field distribution of Fig 5 (a). The tune shift is about 3.7×10^{-5} (2×10^{-5}) within a beam offset of ±10 mm from the axis (on axis).

The beam emittance growth has been evaluated as well by integrating the H-function for the non-achromat lattice [3]. The TPS is operating in the non-achromatic configuration because it has the lowest beam emittance without high field IDs. Generally, the effects of any high field ID should be evaluated before installation. The parameters for the evaluation are an ID length of 0.4 m and a maximum field of 1.8 T for the wiggler to be installed in the 7 m short straight section. The result shows that the emittance will increase by 0.7 % after installation of the W100. Thus, tune shift and emittance increase are very small, because the magnet length is short and the GFR is wide.

Demagnetizing fields must be considered when choosing PM block materials. Figure 7 (a) shows test points for penetrating fields 0.1 mm below the surface of the magnet blocks. Three points, Hcz1, Hcz2 and Hcz3, were checked to ensure that the penetrating field in the magnet are less than the coercivity field of the magnet block material. The components of the penetrating field are calculated and plotted in Fig. 7 (b). For example, label Hcz2z indicates the z-component of the penetrating field at point Hcz2. The strongest fields are 12500 G and -14800 G at points Hcz2z and Hcz1z, respectively. Therefore, the coercivity of the chosen PM material must be larger than 16 kOe or 1273 kA/m (1 T=10 kOe=795.77 kA/m).

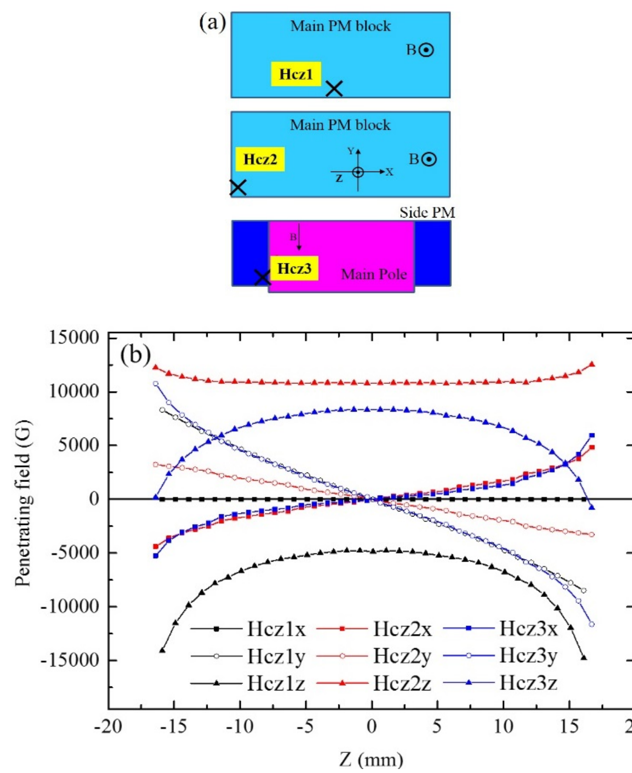

Figure 7: Test points (a) for the penetrating field in the PM block and penetrating field (b) at test points.

SUMMARY

A wiggler magnet (W100) with 1.8 T peak fields has been designed for the X-ray microscopy beamline at the TPS. The magnetic fields were simulated and verified by the RADIA and TOSCA programs. The electron trajectory angle (IBy) and offset (IIBy) are minimized by choosing an even number of main poles and a single pair of end poles, respectively. The dynamic field integral, tune shift and emittance of the electron beam were calculated and found to be very small. The demagnetizing field for the W100 has been calculated as well and it was found that the PM block material must have a coercivity larger than 16 kOe.

Content from this work may be used under the terms of the CC BY 3.0 licence (© 2018). Any distribution of this work must maintain attribution to the author(s), title of the work, publisher, and DOI.

ISBN: 978-3-95450-184-7 doi:10.18429/JACoW-IPAC2018-THPMK013

Content from this work may be used under the terms of the CC BY 3.0 licence (© 2018). Any distribution of this work must maintain attribution to the author(s), title of the work, publisher, and DOI.

REFERENCES

[1] C. C. Kuo *et al.*, "CURRENT STATUS OF LATTICE DESIGN AND ACCELERATOR PHYSICS ISSUES OF THE 3 GeV TAIWAN SYNCHROTRON LIGHT SOURCE", *in Proc. Particle Accelerator Conf. PAC07*, pp. 1085-1087 (2007).

[2] TPS Design Handbook, v16.

[3] H. C. Chao *et al.*, "BEAM DYNAMICS EFFECTSWITH INSERTION DEVICES FOR THE PROPOSED 3 GEV RING IN TAIWANA", *in Proc. APAC'07*, Raja Ramanna Centre for Advanced Technology(RRCAT), Indore, India (2007),pp. 196-198.

[4] J. Safranek *et al.*, "Nonlinear dynamics in a SPEAR wiggler", *Physical Review Special Topics - Accelerators and Beams*, Volume 5, 010701 (2002).